LIMNOLOGY
and
OCEANOGRAPHY: METHODS

ASLO

Limnol. Oceanogr.: Methods 2025

doi: 10.1002/lom3.70018

NEW METHODS

Predicting potential Arctic kelp distribution and lower-depth biomass from seafloor irradiance

Laura Castro de la Guardia [1,2,3]*, **Inka Bartsch** [4], **Haakon Hop** [3], **Sarina Niedzwiedz** [5], **Luisa Düsedau** [4,6], **Nora Diehl** [5], **Dorte Krause-Jensen** [6,7], **Mikael Sejr** [6,7], **Thomas Gjerfluff Ager** [6], **Jean-Pierre Gattuso** [8,9], **Robert W. Schlegel** [8], **Cale A. Miller** [10], **Karen Filbee-Dexter** [11,12], **Pedro Duarte** [3]*

[1]University of the Highlands and Islands, Inverness, UK; [2]Scottish Association for Marine Science, Oban, UK; [3]Norwegian Polar Institute, Fram Centre, Tromsø, Norway; [4]Alfred Wegener Institute, Helmholtz Centre for Polar and Marine Research, Bremerhaven, Germany; [5]Marine Botany, Faculty of Biology and Chemistry & MARUM, University of Bremen, Bremen, Germany; [6]Department of Ecoscience, Aarhus University, Aarhus C, Denmark; [7]Arctic Research Centre, Aarhus University, Aarhus C, Denmark; [8]Sorbonne Université, CNRS, Laboratoire d'Océanographie de Villefranche, Villefranche-sur-mer, France; [9]Institute for Sustainable Development and International Relations (IDDRI-Sciences Po), Paris, France; [10]Department of Earth Sciences, Geoscience, Utrecht University, Utrecht, The Netherlands; [11]University of Western Australia, Perth, Australia; [12]Institute of Marine Research, Nordnes, Bergen, Norway

Abstract

Kelps have an extensive distribution in Arctic coastal waters. However, quantifying their role in the Arctic food web and carbon cycle is challenged by the scarcity of documented geographical distribution, standing stocks and production. Here we present a framework based on an empirical function to predict the potential kelp distribution and their summer biomass as a function of seafloor irradiance and bathymetry. Predictions of biomass were limited to the lower-depth, light-limited range of the kelp distribution, where the fit of the empirical function was significant (from the depth of maximum biomass to the deepest kelp extent). The model was developed and tested in Kongsfjorden, Svalbard, and applied in six additional fjords in the Arctic. The predicted potential kelp biomass in the fjords ranged from 0.6 to 4.7 kg WW m^{-2} and was in good agreement with published values. The resulting kelp standing stock ranged from 0.4 to 300 Gg DW, corresponding to 0.2–109 Gg C. These potential estimates account for light limitation, but do not consider substrata or other factors limiting the kelp distribution area. We identified fjord-specific dependencies between predicted standing stocks and seafloor irradiance and between seafloor irradiance and its drivers (surface irradiance and water column light attenuation) but found no significant change between 2004 and 2022. Our framework provides a baseline for estimating potential kelp biomass from seafloor irradiance, which is expected to change with increasing sediment runoff causing coastal darkening.

Kelps are brown subtidal macroalgae that can form large, vegetated forests in coastal habitats. They are important foundation species and primary producers in the Arctic coastal zone where they support biodiversity, food webs, and carbon cycling like elsewhere in their distribution range (Wernberg et al. 2019). Climate change is transforming benthic coastal habitats across the Arctic (Krause-Jensen et al. 2020; Düsedau et al. 2024a; Sejr et al. 2024). Kelp forests, which largely have a boreal origin in the Northern Hemisphere, are expected to respond positively to projected ocean warming and longer open water periods, especially in areas where these changes

*Correspondence: laura.castrodelaguardia@uhi.ac.uk; pedro.duarte@npolar.no

Associate editor: Tammi Richardson

result in improved conditions for the growth of kelps (Filbee-Dexter et al. 2019; Lebrun et al. 2024). Quantifying changes in Arctic kelp biomass (kg m^{-2}) and standing stocks (total biomass in Gg) remains a challenge due to the scarcity of time series data and limited knowledge of their spatial and depth distribution.

Indeed, actual observations of kelp biomass are largely lacking over most of the Arctic. To date, only two unique datasets stand out: an assessment of kelp and other macroalgae biomass across various ecosystems in Canadian coastal waters (Adey and Hayek 2011), and a multi-year dataset of biomass along a depth gradient collected in Kongsfjorden, Svalbard (Hop et al. 2012a; Bartsch et al. 2016; Düsedau et al. 2024a). Biomass measurements in Arctic coastal waters require skilled diving activities in harsh conditions and with a short seasonal window (Borum et al. 2002; Hop et al. 2012a; Bartsch et al. 2016; Düsedau et al. 2024a). This represents a challenge for continuous monitoring and motivates the search for conceptual frameworks from which observations can be extrapolated.

Spatial mapping of the vertical Arctic kelp distribution has been accomplished in field surveys over small areas (e.g., Kruss et al. 2017; Bluhm et al. 2022; Ager et al. 2023; Castro de la Guardia et al. 2023). At larger scales, the potential suitable habitat for kelps has been mapped using models based on key abiotic variables such as seafloor irradiance, bathymetry (e.g., depth of water column), temperature, and sea ice conditions (e.g., Goldsmit et al. 2021; Assis et al. 2022; Bringloe et al. 2022). These modeling studies, together with the field studies, highlight seafloor irradiance, or photosynthetically available radiation at the seafloor (PAR_b), as the key factor in determining the potential kelp distribution in the Arctic (e.g., Chapman and Lindley 1980; Dunton 1990; Gattuso et al. 2006; Castro de la Guardia et al. 2023). Indeed, PAR_b has long been identified as a key factor for delimiting the vertical distribution of kelp (e.g., Lüning and Dring 1979; Lüning 1991 and reference therein).

PAR_b is also a particularly important variable in the context of climate change because it responds simultaneously to changes in sea ice, cloud cover and water turbidity (Schlegel et al. 2024). In clear Arctic waters, the annually integrated PAR_b ($iPAR_b$) is higher in years with less sea ice as compared to years with more sea ice (Castro de la Guardia et al. 2023). This positive relationship can be offset by increasing water turbidity and cloud cover (Bélanger et al. 2012; Bonsell and Dunton 2018; Laliberté et al. 2021; Düsedau et al. 2024a). Water turbidity increases the light attenuation coefficient of photosynthetically available radiation (K_{dPAR}), thereby reducing PAR_b (Bonsell and Dunton 2018; Düsedau et al. 2024a). Observations across the Arctic, show that water turbidity has overall increased K_{dPAR}, despite the gains in open water days (Singh et al. 2022; Davies and Smyth 2025). Likewise, increases in storm frequency and associated cloud cover due to the Arctic sea ice loss (Wang et al. 2021; Cesana et al. 2024) reduce the PAR reaching the ocean surface and thereby counter potential increases in underwater PAR associated with sea-ice retreat (Laliberté et al. 2021; Bélanger et al. 2012). These developments would suggest a reduction in Arctic kelp biomass.

In this paper, we propose a conceptual framework that can offer an immediate solution to enhance our understanding of the spatial and interannual variability of the potential distribution and biomass of Arctic kelp. The approach is based on an empirical function that links in situ summer data on Arctic kelp community biomass along a depth gradient to satellite-derived $iPAR_b$ at Hansneset, Kongsfjorden, Svalbard. The model is applied to six additional Arctic fjords where high-resolution $iPAR_b$ data was available and used, together with the bathymetry data, to predict the potential kelp distribution area, and summer biomass. The seven selected fjords include a mix of glacial fjords with marine- and land-terminating glaciers, as well as fjords that are no longer glaciated. Here they serve as baselines of the ongoing impact of climate change on Arctic kelp biomass in fjord ecosystems.

Materials and procedures

Bathymetry and irradiance data

Gridded bathymetry and irradiance datasets are from Schlegel et al. (2024) and available at PANGAEA (Gentili et al. 2023, 2024). Schlegel et al. (2024) generated the bathymetry data by merging observed fjord-specific high-resolution bathymetry with the Arctic-focused, 200-m resolution IBCAO version 4.2 bathymetry data of Jakobsson et al. (2020). Therefore, the horizontal grid resolution of the bathymetry data in each fjord is different: 50 m in Kongsfjorden and Porsangerfjorden, 100 m in Young Sound, 150 m in Nuup Kangerlua and 200 m elsewhere (Schlegel et al. 2024).

The irradiance data consist of monthly mean values from 2003 to 2022 for the period of the polar day (May to October). During the polar night (November to April), irradiance was assumed to be near zero. Variables included photosynthetically available radiation just beneath the ocean surface (PAR_{0-}), euphotic-zone-averaged K_{dPAR}, and PAR_b (Schlegel et al. 2024). The ocean color data used to generate the irradiance data were based on the top-of-atmosphere radiance from MODIS-Aqua level-1A (L1A) data ($\sim$ 1 km daily resolution). The L1A data were then processed to level 2 using SeaDAS v8, while maintaining the native resolution of 1 km. K_{dPAR} was determined as a function of the absorption and backscattering coefficients (i.e., inherent optical properties) of the water column and the solar zenith angle (Singh et al. 2022). A detailed discussion on how this conversion was made accurately for the high latitude Arctic regions, including our seven fjords, is provided in section 2.3 of Schlegel et al. (2024). PAR_b was downscaled to the high spatial resolution of the bathymetry data in each fjord by applying the Beer–Lambert Law ($PAR_b = PAR_{0-} \times e^{-K_{dPAR} \times seafloor\_depth}$), where seafloor depth is extracted from the high resolution bathymetry and the parameters K_{dPAR} and PAR_{0-} are used at their native 1 km pixel resolution (more details in section 2.4 of Schlegel et al. 2024). In

summary, these data combine satellite-based information on surface irradiance, affected by insolation and sea-ice cover, and K_{dPAR} affected by turbidity due to runoff and glacial melt (Schlegel et al. 2024).

We estimated $iPAR_b$ by multiplying the original monthly mean PAR_b data by the number of days in each month, integrating over each year, and applying a running mean filter with a 2-yr window length to create a time series from 2004 to 2022. The 2-yr window was chosen to reflect the recruitment modes of kelp, which influence the standing stock of blade material and the elongation of stipes (in Greenland fjords, Borum et al. 2002; Krause-Jensen et al. 2020; in Svalbard and Norway, Lüning 1991). Therefore, the $iPAR_b$ time series from 2004 to 2022, accounts for the cumulative light conditions over the current and previous year and thus is considered representative of the cumulative irradiance contributing to the kelp blade and stipe biomass used in developing the empirical model from which we derived the biomass.

Measured kelp community biomass data

The kelp community biomass was measured as the summed biomass of the three common kelps at Hansneset in Kongsfjorden: *Alaria esculenta*, *Saccharina latissima*, and digitate kelps (consisting of *Laminaria digitata* and *Hedophyllum nigripes*). The biomass of these species was sampled along the depth gradient in multiple years: 1996–1998 (Hop et al. 2012b), in 2012–2013 (Bartsch et al. 2016), and in 2021 (Düsedau et al. 2024b). These species are particularly relevant as they consistently dominate macroalgal cover at higher latitudes (Adey and Hayek 2011; Wegeberg et al. 2025).

We use kelp biomass in units of dry weight (DW) g m^{-2}. We converted wet weight (WW) to units of DW by dividing by the ratio of WW to DW in Kongsfjorden of 7.3 for *S. latissima*, 5.8 for *A. esculenta*, 6.1 for *L. digitata* (Bartsch et al. 2016). However, the WW to DW ratio varies to some extent in the literature, with other studies in Kongsfjorden suggesting ratios for the same three species of 7.9, 6.7, and 6.1, respectively (Düsedau et al. 2024a) and 6.0, 3.8, and 7.4, respectively (Miller et al. 2024). In Nuup Kangerlua fjord, Greenland the WW to DW ratio was 7.3 for all Laminariales (Ager et al. 2023), and in fish farms in southern Norway 60°N it was 6.6 for *S. latissima* (Fossberg et al. 2018). The variability in the WW to DW ratios can be partially attributed to the time of sampling and differences in field methodologies for measuring WW. For instance, some studies (e.g., Bartsch et al. 2016; Düsedau et al. 2024a) use cotton towels to remove water and epibiota from the kelp surface, whereas others focus solely on removing epibiota or only shake the kelp blades for a certain amount of time. The less water or epibiota removed, the higher the ratio becomes.

Empirical framework to predict kelp distribution and biomass

We use a three-step approach to estimate the kelp standing stocks within the lower depth range of the kelp distribution. The lower depth range is defined as the portion of the distribution extending from the depth of maximum biomass to the deepest limit of kelp occurrence. The model framework is illustrated in Fig. 1 and each step is described in the following subsections. The schematic illustrates our consideration for the spatial variability of $iPAR_b$ along a fjord's coastline and emphasizes the differences in key processes that affect $iPAR_b$ (e.g., sectors c1–c5 in Fig. 1): in sector (c1) a dense sediment plume and/or ice shading limits irradiance across the full depth range; in sector (c2) ice shading near the coast limits irradiance only in the upper depth range; in sector (c3) ice shading offshore limits irradiance in the lower depth range and shallows the kelp depth limit; in sector (c4) same as sector (c3) but with longer ice duration, further shallowing the kelp depth limit; in sector (c5) the steep terrain (e.g., bathymetry) limits irradiance across much of the lower depth range.

Step 1: Predicting the kelp distribution area based on $iPAR_b$

We applied an $iPAR_b$ threshold to define the horizontal and vertical extent of kelp distribution within the fjord. Each pixel in the model grid was classified into a binomial outcome: kelp presence ($iPAR_b \geq 47$ mol photons m^{-2} yr^{-1}) or kelp absence ($iPAR_b < 47$ mol photons m^{-2} yr^{-1}). This threshold is chosen because several studies have consistently demonstrated that $iPAR_b \geq 47$ mol photons m^{-2} yr^{-1} defines the compensation light of Arctic kelp and the depth extent of the kelp forests (e.g., Chapman and Lindley 1980; Dunton 1990; Krause-Jensen et al. 2019; Castro de la Guardia et al. 2023). The potential kelp distribution was delineated by the pixels classified as kelp presence.

Limitations of predicting kelp distribution using $iPAR_b$ threshold

The predicted kelp distribution assumes 100% kelp cover over the areas that are not light limited; it does not consider substrata limitations or biological interactions. Consequently, it should be regarded as a maximum potential extent of the kelp habitat within each fjord.

Substratum is of primary importance for kelps, which typically grow attached to rocks or other hard substrata. Kelps prefer hard or mixed substrata (e.g., with dropstones) over soft sediments, such that in the presence of soft sediments kelp may not grow even when light conditions are optimal (e.g., Hop et al. 2016; Kruss et al. 2017; Bluhm et al. 2022). Rocky seafloor in front of retreating marine-terminating glaciers, for example, has higher kelp cover than soft-bottom seafloor near river outflows (Gonzalez Triginer et al. 2024). Unfortunately, the substrata along the coastlines of these seven Arctic fjords are largely unknown. A reasonable assumption is that the proportion of soft sediments is moderate to high, as documented elsewhere in the Arctic (Filbee-Dexter et al. 2022; Bluhm et al. 2022; Wegeberg et al. 2025). In soft substrata coastlines, boulders and small pebbles within the soft sediments can provide a surface for attachment and allow the successful growth of some, but not all kelp species

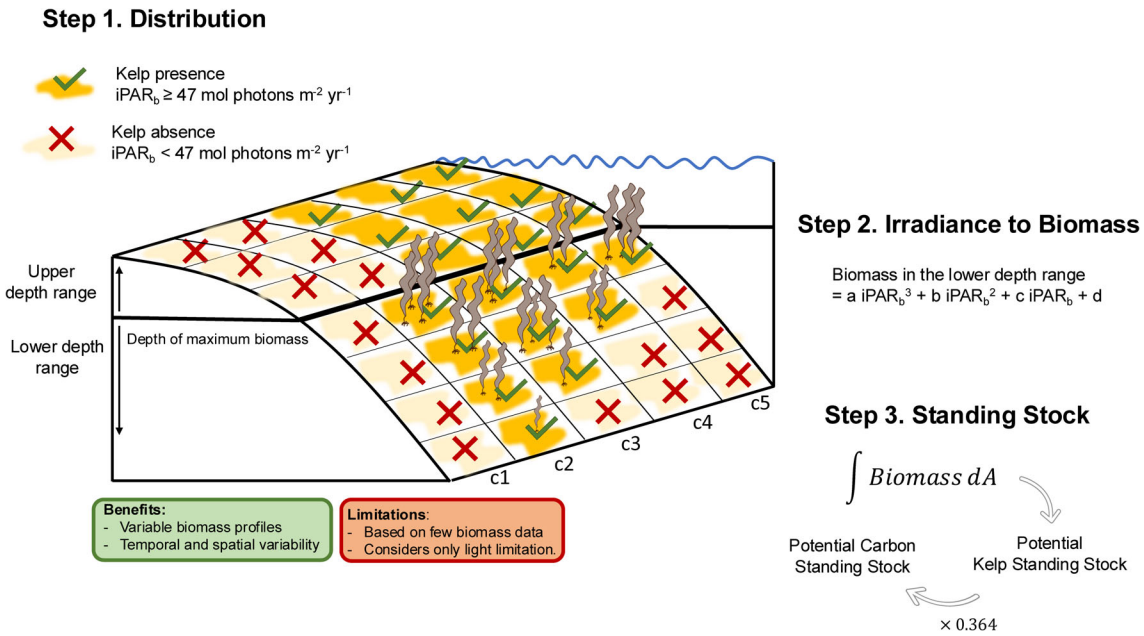

Fig. 1. A three-step approach to estimate the kelp distribution, summer biomass and summer standing stocks using iPAR$_b$. The methodology for each step is described in the text. Step 1 predicts the potential distribution of kelp over the full depth range. Steps 2 and 3 focus on predicting potential biomass and standing stock within the lower depth range. In Step 3, the biomass is integrated over the area (A) of the lower depth range. Each sector (c1–c5) represents an example zone where different physical processes affect light penetration to the seafloor.

(e.g., *S. latissima*, *Laminaria solidungula*; Borum et al. 2002; Hop et al. 2016; Filbee-Dexter et al. 2022; Castro de la Guardia et al. 2023). The percentage cover of kelp, however, will still be restricted by the density of the boulders (Borum et al. 2002; Krause-Jensen et al. 2007). In Young Sound, for example, the lack of hard substrata forces *S. latissima* to attach to pebbles that do not allow the development of a dense, multi-layered canopy (D. Krause-Jensen pers. comm.).

Sea urchin grazing represents another significant factor to consider in constraining our predicted kelp distribution. Intensive grazing can result in the creation of sea urchin barrens in otherwise habitable regions (Christie et al. 2019; Ager et al. 2023). Some fjords may be more vulnerable to grazing than others. Sea urchin grazing has been confirmed in Kongsfjorden, Disko Bay, Nuup Kangerlua and Porsangerfjorden affecting depths ranging from 0 to 50 m (Krause-Jensen et al. 2019; Molis et al. 2019; Ager et al. 2023; Hop et al. 2025). Sea urchin grazing in Kongsfjorden has also resulted in some barren grounds (Molis et al. 2019), particularly in the outer part of the fjord where sea urchins are abundant (Hop et al. 2025). In these areas, grazing is depth related and has become most severe in the deepest part of the forest (e.g., > 10 m depth). It is difficult to predict grazing areas because information on the biological drivers is not readily available in the Arctic. There are also more complex interactions between physical environmental factors (like sedimentation) and grazing pressure: grazing pressure may decrease due to the lower quality of kelp (as it becomes covered in sediment), or grazers may shift their grazing patterns to areas with less sediment impact (Traiger et al. 2019). Grazing pressure may also decrease with rising temperature and ocean acidification (Brown et al. 2014).

Several additional physical factors such as sea-ice scouring, wave action, sedimentation rates, and tidal range can restrict the kelp distribution (e.g., Mohr et al. 1957; Lüning 1991; Wiencke and Amsler 2012; Krause-Jensen et al. 2020; Filbee-Dexter et al. 2022; Kvile et al. 2022). Particularly, fjord coastal habitats are prone to high sedimentation which may hinder successful colonization of kelp, keeping biomass low (Zacher et al. 2016). Moreover, the spatial distribution of kelp in the Arctic is influenced by multiple interactions between abiotic factors. Using the example of the temperate kelp *Laminaria hyperborea*, it has been shown that the interaction between photoperiods (length of polar day and polar night) and ocean warming plays a crucial role in determining its potential for northward expansion (Diehl et al. 2024).

Evaluation of the predicted kelp distribution area

To evaluate the ability of iPAR$_b$ threshold to predict the kelp distribution area we constructed a dataset of GPS locations with data on the presence and absence of kelp reported in the literature (Table S1). Ninety-nine percent of all GPS locations are from the extensive macroalgae monitoring activities, including diving and acoustic surveys, conducted in Kongsfjorden (e.g., Hop et al. 2012b; Bartsch et al. 2016; Kruss et al. 2017; Schimani et al. 2022; Düsedau et al. 2024b; C. A. Miller pers. comm.) and Isfjorden (Gonzalez Triginer

et al. 2024), while in the other five fjords there are only small-scale surveys resulting in fewer GPS locations.

In Kongsfjorden, we gathered a total of 414,023 GPS locations, and kelp presence was confirmed at 3868 of these locations. We defined the presence of kelp on GPS locations derived from the acoustic survey following Kruss et al. (2017) criteria: ping number between 1 and 350, and canopy height ≥ 0.28 m; otherwise, kelp was considered absent from that GPS location. In Isfjorden, there were a total of 3444 locations with estimates of the percentage cover of kelp. In this case, kelp presence was defined at GPS locations with a percentage cover ≥ 10% and absence as < 10%. Presence of kelp was confirmed at 2202 GPS locations in Isfjorden. In Nuup Kangerlua, we gathered 35 GPS locations with estimates of percentage cover of kelp; presence of kelp was confirmed at 33 locations (T. G. Ager pers. comm.). In addition, we gathered 9 GPS locations with confirmed presence of kelp in Disko Bay (*Laminaria* and *Saccharina* species, Krause-Jensen et al. 2019), 3 GPS locations with confirmed presence of kelp in Porsangerfjorden (L. Düsedau and F. Filbee-Dexter pers. comm.) and 1 GPS location with confirmed presence of kelp in Young Sound (Borum et al. 2002).

Observed GPS locations with presence and absence of kelp were interpolated onto our model grid using the nearest neighbors. The evaluation consisted of overlapping these observations with our predictions to quantify the instances in which our model accurately predicted kelp presence and absence based on $iPAR_b$ threshold. We report standard binary classification metrics, including overall predictive accuracy (%), recall (true positive rate), and specificity (true negative rate).

While the focus of step 1 was on predicting the full extent of the kelp distribution area, the focus of steps 2 and 3 is on the lower depth range of kelp distribution, where kelps are light-limited, and their biomass can be predicted using the empirical light model described in Step 2.

Step 2: Potential summer biomass in the lower depth range of the kelp distribution

At Hansneset, Kongsfjorden, the observed summer kelp biomass follows a bell-shaped curve when plotted as a function of depth (Fig. S1a) and $iPAR_b$ (Fig. S1b). In each sampling year, the kelp biomass increased from the infralittoral fringe (approx. depth 0 m) toward a biomass maximum with increasing depth and decreasing $iPAR_b$. The depth of the biomass maximum was 5 m in 1996/98 and 2.5 m in 2012/2013 and 2021, and $iPAR_b$ at the biomass maximum was 537, 1360, and 885 mol photons m^{-2} yr^{-1} in 1996/98, 2012/13 and 2021 respectively. Below the biomass maximum, the kelp biomass decreased with increasing depth and further decreasing $iPAR_b$. At a depth of 15 m, biomass and $iPAR_b$ were close to zero (Fig. S1).

These bell-shaped curves of biomass as a function of depth and $iPAR_b$ suggested that we can divide the data into two groups: (1) biomass in the upper depth range, from the infralittoral fringe down to the depth of maximum biomass (not inclusive) and (2) biomass in the lower depth range, from the depth of maximum biomass to the deepest limit of the kelp forest. Spearman's rank-order correlation (r_s) was used to measure the strength of the monotonic relationship between irradiance and biomass in the upper and lower depth ranges. Only the kelp biomass in the lower depth range had a significant monotonic correlation with the gradient in $iPAR_b$ (lower depth range: $r_s = 0.93$; $p < 0.05$ vs. upper depth range: $r_s = -0.31$; $p = 0.56$). Therefore, the empirical function to derive summer biomass from seafloor irradiance was developed using data from the light-limited lower depth range.

The cubic function (equation in Fig. 2) predicts summer biomass gDW m^{-2} as a function of $iPAR_b$ mol photons m^{-2} yr^{-1} in the lower depth range. The cubic function provided the best fit to the observed data among the set of tested models (Table S2). Model selection was based on root mean square error (RMSE), with the lowest RMSE indicating the highest predictive accuracy.

The cubic model was constructed using the multiyear summer biomass dataset from Bartsch et al. (2016) and Düsedau et al. (2024b). Its robustness was evaluated by refitting the model with six additional data points from Hop et al. (2012b). In the case of Hop et al. (2012b), where the biomass sampling years (1996/98) preceded the start of our $iPAR_b$ time series, we used data from 2004, the earliest year in our time series $iPAR_b$. The relationship between $iPAR_b$ and the biomass of the Arctic kelp community in the lower depth range was strong (adjusted coefficient of determination $R^2_{adj} = 0.86$, RMSE = 221.8 gDW m^{-2}, *F*-statistic, $F_{3,4} = 15.7$). Refitting the model with the additional data showed that the relationship improved with more data ($R^2_{adj} = 0.90$, RMSE = 183 gDW m^{-2}, $F_{3,10} = 41.6$). However, the Akaike Information Criterion (AIC) and Bayesian

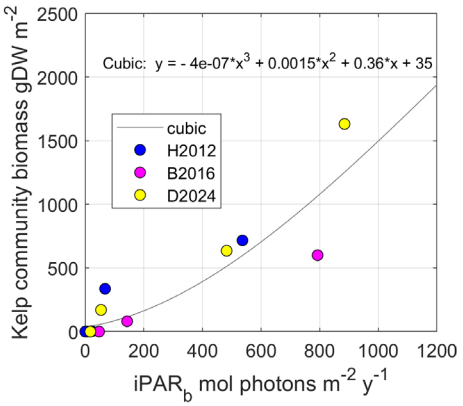

Fig. 2. Empirical relation between $iPAR_b$ and the Arctic kelp community summer biomass in the lower depth range. Kelp biomass data is from Hansneset, Kongsfjorden, Svalbard in 1996/98 (Hop et al. 2012b: H2012), 2012/13 (Bartsch et al. 2016: B2016) and 2021 (Düsedau et al. 2024b: D2024).

Information Criterion (BIC) remained stable (ratios of 1 and 0.99, respectively), supporting the reliability of the relationship between $iPAR_b$ and kelp biomass across a broader dataset and demonstrating the robustness of the original model.

To apply the empirical model to predict summer kelp biomass in the lower depth range, we must first identify the depth of maximum biomass, which defines the upper limit of the lower depth range (Table 1). In Kongsfjorden and Young Sound, the depth of maximum biomass is based on published biomass data along the depth gradient. In other fjords, such data are not available. However, we found that the depth of maximum biomass and the depth of maximum kelp percentage cover are the same in Kongsfjorden and Young Sound (Table 1). We assume the same applies to other fjords and used maximum percentage kelp cover as a proxy of maximum biomass in the fjords without biomass data. In these fjords, we defined the upper limit of the lower depth range of kelp distribution as the depth of maximum percentage cover.

Limitations of the empirical irradiance-to-biomass function

By considering only a few kelp groups (*A. esculenta*, *S. latissima*, and digitate kelps), the empirical model may not adequately reflect the complexity of the kelp community. In many Arctic regions, the kelp communities are formed by a larger macroalgal assemblage (e.g., Dunton et al. 1982; Makarov 1998; Plotkin et al. 2005; Tatarek et al. 2012; Ronowicz et al. 2020; Sejr et al. 2021). Therefore, our predicted kelp biomass may underestimate the overall kelp forest community biomass. On the other hand, the model may overestimate the kelp biomass in regions where there is only one common kelp species, or in regions where, at any given depth, the kelp biomass is more closely related to hard substrata availability than to seafloor irradiance such as for *S. latissima* in Young Sound (Borum et al. 2002; Krause-Jensen et al. 2007).

The depth of maximum kelp biomass or percentage cover (Table 1) is a key parameter in our model for estimating potential kelp community biomass. This depth varies naturally across space due to factors such as wave exposure, sea-ice cover, tidal activity, and substrate type, and it is both species- and climate-dependent. In the present model, we assumed this depth to be constant, using the mean value within each fjord and, when available, the most recent estimate from temporal datasets. The model is particularly sensitive to this parameter, as even small changes in the depth of maximum biomass can cascade into large differences in estimated biomass. For example, the depth of maximum cover in Kongsfjorden, shallowed from 5 to 2.5 m between 2012 and 2016 (Fig. S1). Using the most recent value of 2.5 m doubles the predicted biomass and increases the potential habitable area in the lower depth range by 13 km^2 compared with using 5 m. This sensitivity highlights a key limitation of the model, as spatial and temporal variability in the depth of maximum cover is not yet resolved.

Step 3: Calculating kelp standing stock (DW and C units)

The third step predicts the potential kelp standing stocks (Gg DW) in summer by integrating the modeled kelp community biomass in the lower depth range of the kelp distribution in each fjord, assuming 100% kelp cover. To express the potential kelp standing stock in carbon units (Gg C), we multiply the kelp standing stock DW by the observed ratio of carbon/DW of 0.364 (Krause-Jensen et al. 2012). This ratio was used as an approximation, considering that the carbon/DW ratio may vary between macroalgae species (range 0.1–0. 5; Duarte 1992). By using the overall kelp community biomass, and just one conversion factor, we also do not consider interspecific diversity, which could potentially yield a more refined carbon estimate (Wright et al. 2022), but this is beyond the scope of this study.

We use the non-parametric Mann–Kendall test with Theil–Sen regression to estimate the trend 2004–2022 in the potential standing stock, $iPAR_b$, PAR_b, K_{dPAR}, and PAR_{0-}. We use the Generalized Additive Model (GAM) to quantify how much of the variance in $iPAR_b$ and PAR_b is explained by its predictors PAR_0, K_{dPAR}. We fit models using MATLAB's *fitrgram* with default smoothing parameters and random initialization to ensure stability. We evaluate model performance with the

Table 1. Observed depth (m) of maximum kelp biomass and maximum kelp percentage cover in the seven fjords in summer. Not available data is identified as n/a.

	Depth of maximum kelp biomass (m)	Depth of maximum kelp cover (m)	Source
Young Sound	10	10	Borum et al. 2002; Krause-Jensen et al. 2007
Kongsfjorden	2.5	2.5	Bartsch et al. 2016; Düsedau et al. 2024b
Storfjorden	n/a	6	Wiktor Jr et al. 2022
Isfjorden	n/a	5	Wiktor Jr et al. 2022; Gonzalez Triginer et al. 2024
Porsangerfjorden	n/a	6	L. Düsedau and K. Filbee-Dexter pers. comm.
Nuup Kangerlua	n/a	10	Ager et al. 2023
Disko Bay	n/a	5	D. Krause-Jensen pers. comm.

coefficient of determination (R^2) and quantify the predictor dominance as the reduction in performance when the predictor is omitted.

The accuracy of the predicted value of potential standing stock is limited by the model's dependence on predicted kelp distribution and biomass, so any uncertainties in those earlier steps, propagate through to the final prediction of potential standing stock.

Assessment and results

Predicted kelp distribution area

The predicted extent of the total kelp distribution area varied widely between fjords (*see* total kelp extent in Table 2). The total kelp extent ranged from < 100 km^2 in Kongsfjorden, Young Sound, and Porsangerfjorden, to hundreds of km^2 in Storfjorden, Nuup Kangerlua and Isfjorden, to over 2000 km^2 in Disko Bay. The predicted total extent of the kelp distribution was 10% of the fjord area, except in Porsangerfjorden where it was only 2%, and in Nuup Kangerlua where it was 20% (ratio of total extent to fjord area in Table 2). This was influenced by the coastal morphology, whereby narrow fjords with shallow shelves, such as Nuup Kangerlua, tended to have more favorable irradiance conditions, and thus larger predicted total kelp extent to fjord area, compared to fjords with steep banks, such as Porsangerfjorden (Fig. S2).

The predicted extent of the lower depth range was 46 ± 26% of the total kelp distribution area. The depth distribution of the lower depth range also varied between fjords (Fig. S3). In Kongsfjorden the lower depth range extended from 2.5 to 22 m, with over 50% of the modeled kelp pixels occurring between 2.5 and 8 m (Fig. S3a). In Young Sound, the lower depth range extended from 10 to 16 m depth, with over 50% of the kelp pixels occurring between 10 and 12 m (Fig. S3b). In Porsangerfjorden, it extended from 6 to 30 m, with over 50% of the kelp pixels occurring between 10 and 20 m (Fig. S3c). In Isfjorden, it extended from 5 to 26 m, with over 50% of the kelp pixels occurring between 5 and 10 m (Fig. S3d). In Nuup Kangerlua, it extended from 10 to 34 m, with over 50% of the kelp pixels occurring between 10 and 18 m (Fig. S3e). In Storfjorden, it ranged from 6 to 30 m, with over 50% of the kelp pixels occurring between 6 and 12 m (Fig. S3f). In Disko Bay, it extended from 5 to 31 m, with over 50% of the kelp pixels occurring between 5 and 12 m (Fig. S3g).

Evaluation of the predicted kelp distribution

The accuracy of the kelp distribution in Kongsfjorden, Isfjorden and Nuup Kangerlua was evaluated against GPS locations with kelp presence and absence (Table S1). The accuracy ranged between 41% and 58%, indicating moderate performance across the three fjords. This was primarily driven by the limitations of the $iPAR_b$ threshold model in predicting kelp absences, as reflected in the generally low specificity (Table 3). Low specificity indicated that the model incorrectly predicted kelp presence at locations where it was absent (e.g., a large number of false positives). The model demonstrated high recall, indicating its strong ability to identify kelp presence. Nuup Kangerlua was an exception, with low recall and high specificity rates; though here, the model's evaluation may be limited by the small sample size ($n = 35$) compared to over 1000 locations in the other two fjords (Table 3).

In Disko Bay, Porsangerfjorden, and Young Sound we evaluated the model using a small set of GPS locations with kelp presence. The model predicted 100% of the observations with kelp: 9 in Disko Bay, 3 in Porsangerfjorden, and 1 in Young Sound. There were no data to estimate specificity in these fjords. Finally, no published kelp surveys with GPS locations existed for Storfjorden.

Summer kelp biomass and standing stocks in the lower depth range

Biomass predictions using $iPAR_b$ were limited to the lower depth range. However, for the purpose of visualization, we also plotted in Fig. 3 the predicted kelp distribution in the upper depth range (green) even though we were unable to estimate the biomass in this depth range. The upper depth range was extensive in all fjords, and particularly in Disko Bay, Young Sound, and Nuup Kangerlua, where the extent of the upper depth range accounted for 90 to 70% of the total

Table 2. Fjord area, extent of the total kelp distribution and extent of the lower depth range averaged 2004–2022 (mean ± standard deviation). The ratio of total extent to fjord area, and lower depth range to total extent is also given.

Fjord name	Fjord area (km^2)	Total kelp extent (km^2)	Lower depth range (km^2)	Ratio of total extent/ fjord area	Ratio of lower depth/ total extent
Young Sound	375	39 ± 2	5 ± 1	0.1	0.1
Kongsfjorden	323	36 ± 3	31 ± 2	0.1	0.8
Storfjorden	9008	551 ± 58	343 ± 55	0.1	0.6
Isfjorden	3170	294 ± 15	138 ± 13	0.1	0.5
Porsangerfjorden	2982	70 ± 4	50 ± 4	< 0.1	0.7
Nuup Kangerlua	3786	608 ± 9	166 ± 11	0.2	0.3
Disko Bay	31,878	2290 ± 26	536 ± 23	0.1	0.2

Table 3. Performance metrics of the binary classification method to predict kelp presence and absence based on $iPAR_b$ threshold. The table shows the total number of GPS locations evaluated, the number of observed kelp presence and absences, along with the resulting model accuracy, recall, and specificity. Recall measures the model's ability to correctly predict kelp presence and specificity measures the ability to correctly predict absence.

Fjord	Total locations	Presence locations	Absence locations	Accuracy (%)	Specificity (%)	Recall (%)
Kongsfjorden	414,023	3868	410,155	41	41	78
Isfjorden	3444	2202	1242	58	51	62
Nuup Kangerlua	35	24	11	46	73	33

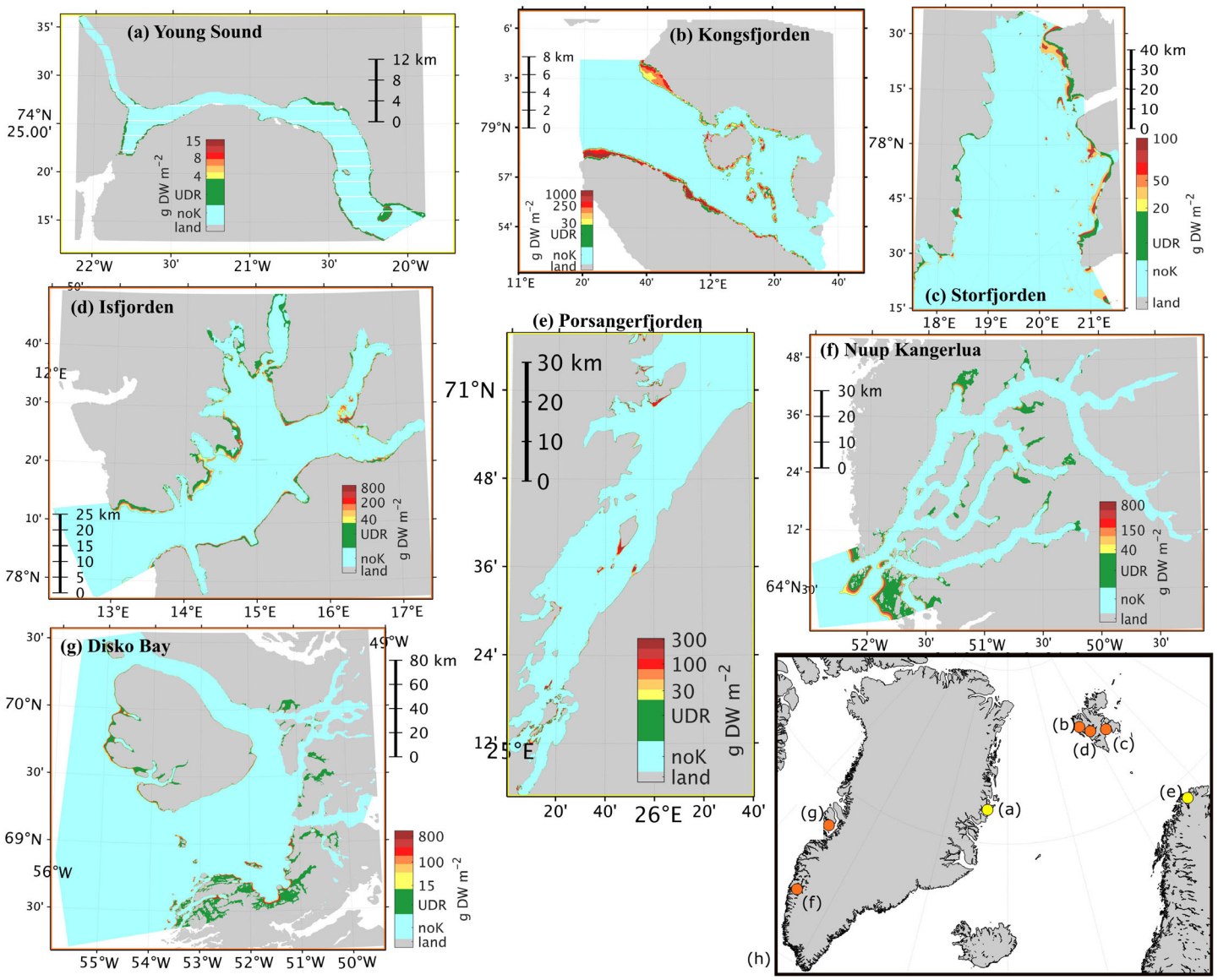

Fig. 3. Predicted kelp presence in the upper depth range (UDR; colored green) and predicted kelp summer biomass in the lower depth range (colored yellow to red). Note the different scales in each panel. Fjords with marine-terminating glaciers and predominantly subglacial discharge are outlined in orange while fjords with predominantly land surface runoff are outlined in yellow in the lower right panel. Areas with below-optimal irradiance where no kelp was predicted (noK) are colored blue. Presenting averages between 2004 and 2022.

kelp distribution area (*see* ratio lower depth range to total extent in Table 2).

The distribution and magnitude of kelp biomass in the lower depth range varied considerably between and within fjords (Fig. 3). The spatial differences in the temporally averaged summer biomass between 2004 and 2022 ranged from as low as 0–15 g DW m^{-2} in Young Sound to over 1000 g DW m^{-2} in Kongsfjorden. The kelp biomass was higher in the outer and mid fjord relative to the inner fjord, with two exceptions: in Porsangerfjorden where the kelp biomass was fragmented and confined to pockets dispersed throughout the fjord, and in Storfjorden where the kelp biomass was higher in the inner fjord. This distribution of biomass generally aligned with the bathymetry in each fjord; in particular, the availability of broad shallow areas (Fig. S2).

The spatial mean potential summer biomass in the lower depth range averaged between 2004 and 2024 was relatively low in Young Sound and Storfjorden (< 1 kgWW m^{-2}), moderate in Nuup Kangerlua, Porsangerfjorden and Isfjorden (~ 2 kgWW m^{-2}), and high in Kongsfjorden and Disko Bay (> 4 kgWW m^{-2}; Fig. 4). The temporally averaged potential summer standing stock mirrors the potential summer biomass predictions in each fjord, with the lowest potential standing stocks in Young Sound and Storfjorden (< 1 Gg DW) and highest in Kongsfjorden and Disko Bay (> 200 Gg DW). These differences among fjords also scaled with the extent of the lower depth range, being smallest in Young Sound and largest in Disko Bay (Fig. 4; Table 2).

The potential cumulative kelp standing stock in the lower depth range of all seven fjords was estimated at 462.3 Gg DW, equivalent to 168.3 Gg C allocated in the living kelp (adding up the standing stock predictions in Fig. 4). As anticipated, due to the disproportionately large extent of the lower depth range in Disko Bay, this region contributed 70% of the cumulative potential standing stocks (Fig. 4). However, Kongsfjorden had the highest potential biomass per area.

Variations in kelp potential standing stocks in the lower depth range area (2004–2022)

There were no trends in the potential summer standing stock in the lower depth range of the seven Arctic fjords between 2004 and 2022 (Fig. 5a–g). Noticeably, there was relatively large interannual variability in the kelp standing stock in all fjords, largely reflecting the variability in regionally averaged $iPAR_b$ within the same area (black in Fig. 5h–n). This correspondence is expected because standing stock was derived directly from $iPAR_b$ (Fig. 1), as a 2-yr rolling mean of annually integrated PAR_b. Consequently, the interannual variability in standing stock and $iPAR_b$, closely paralleled that of annually integrated PAR_b (gray in Fig. 5h–n) and its predictors, PAR_{0-} (green) and K_{dPAR} (purple). There were also no trends in $iPAR_b$ nor the regionally- and annually-averaged PAR_{0-}, PAR_b, and K_{dPAR} between 2004 and 2022.

Annual mean PAR_{0-} in the lower depth range was relatively high (> 22 mol photons m^2 d^{-1}) in fjords south of 72°N, Nuup Kangerlua, Disko Bay and Porsangerfjorden. In contrast, in fjords at higher latitudes, the annual mean PAR_{0-} rarely exceeded 15 mol photons m^2 d^{-1}, corresponding to longer polar night and ice-covered periods. In all fjords the regional and annual mean K_{dPAR} was between 0.25 and 0.30 m^{-1}; only

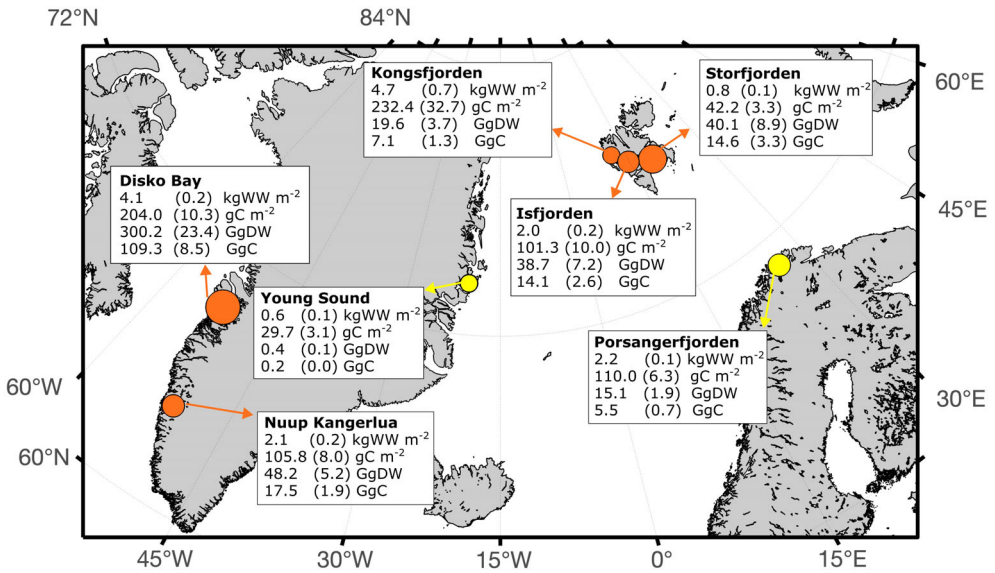

Fig. 4. Predicted potential summer kelp biomass and standing stock in the lower depth range of seven Arctic fjords using the approach described in Fig. 1. Kelp dry weight (g DW) was converted to carbon (C) using a C to DW ratio of 0.364 (Krause-Jensen et al. 2012). Presenting regional and temporal (2004–2022) averages (± standard deviation). Fjords with marine terminating glaciers and predominantly subglacial discharge are indicated with orange circles while fjords with predominantly land surface runoff are indicated by yellow circles. Size of the marker represents the relative extent of the lower depth range (Table 2).

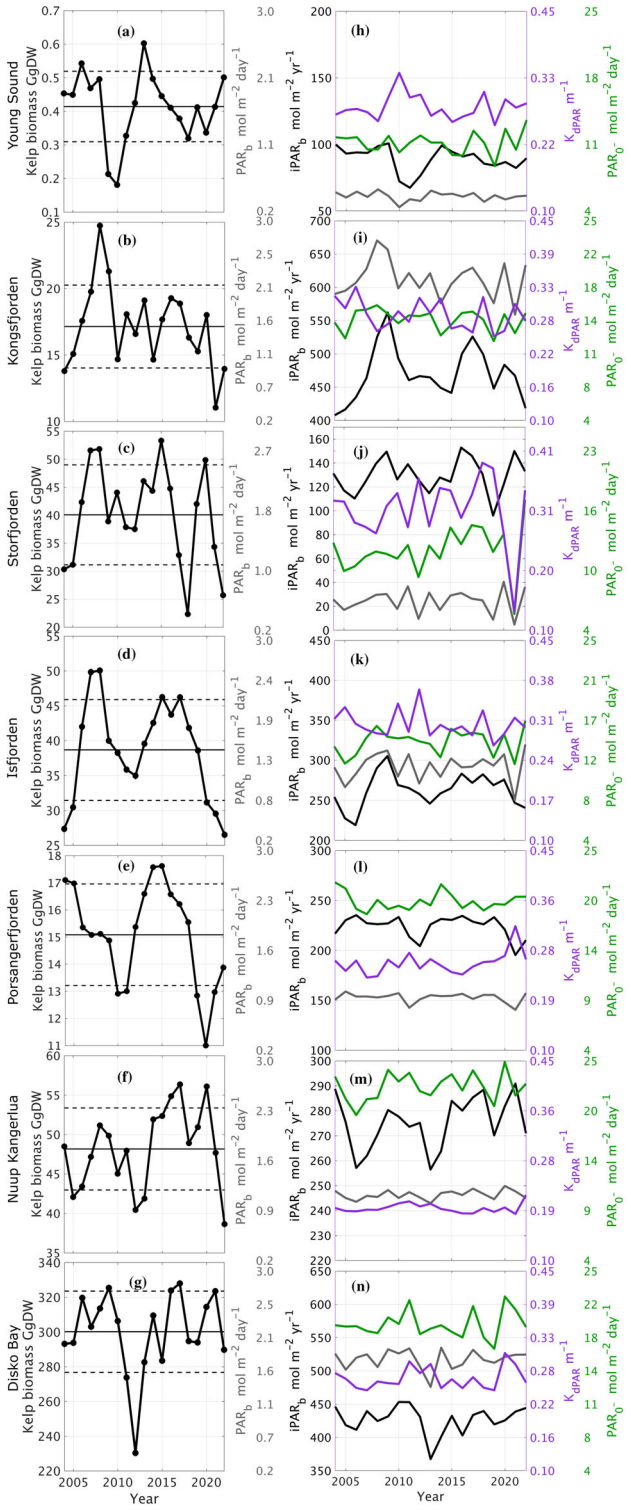

Fig. 5. (**a**–**g**) Fjord-integrated potential summer kelp standing stock within the lower depth range from 2004 to 2022 (solid black line with dots), overlaid by the period mean ± 1 standard deviation (parallel solid and dashed black lines, respectively). (**h**–**n**) Annually- and regionally averaged PAR_b (gray line), $iPAR_b$ (black line) and their predictors, PAR_{0-} (green line) and K_{dPAR} (purple line) from 2004 to 2022. $iPAR_b$ is a 2-yr running mean of the annually integrated PAR_b.

in Nuup Kangerlua was the annual mean K_{dPAR} consistently $< 0.25\ m^{-1}$, an indication of relatively clearer waters.

We found different relationships between the dependent variable $iPAR_b$, and its predictors K_{dPAR} and PAR_{0-} (Fig. 5). Generalized Additive Models explained a large portion of the interannual variability in $iPAR_b$ across the seven fjords ($R^2 = 0.89$–0.99; Table 4) and confirmed that in six out of the seven fjords, PAR_{0-} dominated (57–77%) relative to K_{dPAR} (23–43%). In Young Sound, K_{dPAR} dominated (68%) while PAR_{0-} contributed less (32%). These results indicated that surface irradiance generally exerts the strongest control on $iPAR_b$. Applying the same analysis to the annually averaged PAR_b (Table S3), yielded similarly strong GAMs ($R^2 = 0.88$–0.99) that indicated a stronger dominance of PAR_{0-} (61–85%) relative to K_{dPAR} (18–39%) across most fjords (five of seven). The two exceptions were Young Sound and Isfjorden where K_{dPAR} dominated (68% and 72%, respectively) over PAR_{0-} (32% and 28%).

Discussion

Kelp forests play a pivotal role in the functioning of coastal ecosystems, affecting coastal biodiversity, their food webs and carbon dynamics (e.g., Steneck et al. 2002; Duarte et al. 2005; Krause-Jensen and Duarte 2016; Teagle et al. 2017). The observed warming and loss of sea ice in Arctic coastal habitats motivates a need for mapping and monitoring of the northern kelp forest ecosystems (Krause-Jensen et al. 2020). Here we propose a novel method to predict potential kelp distribution across the full depth range, as well as summer biomass and standing stocks within the lower depth range of seven Arctic fjords using $iPAR_b$. While previous studies have used seafloor PAR to estimate suitable benthic habitats for primary producers (Gattuso et al. 2006; Attard et al. 2024) and benthic primary production in the Arctic (Attard et al. 2024), our method uniquely predicts temporal, spatial, and vertical variations in potential summer kelp biomass. It is based on an empirical relationship between $iPAR_b$ and summer biomass offering an alternative to the common practice of estimating standing stocks by multiplying kelp distribution area by a global average macroalgal production/biomass (Ager et al. 2023; Attard et al. 2024).

The irradiance-to-biomass model presented here is specific to the Arctic kelp community; however, the framework can be broadly applied to temperate and tropical systems, where kelp survival and productivity also correlate with annual cumulative irradiance (Graham et al. 2007; Franke et al. 2023). However, it should be noted that unlike in the Arctic where kelps are exposed to polar day and polar night, kelps in non-polar regions are better acclimatized to year-round daylight cycles. Episodic light fluctuations (e.g., driven by storms, or turbidity) can thus, play a more significant role in controlling kelp productivity and biomass in temperate regions (Smale et al. 2020; Franke et al. 2023) and limit the predictive value of $iPAR_b$.

Table 4. Generalized Additive Model goodness of fit (R^2) and relative influence of PAR_{0-} and K_{dPAR} on the interannual variability in $iPAR_b$.

Fjord name	R^2	K_{dPAR} (%)	PAR_{0-} (%)	Dominant driver
Young Sound	0.95	68.3 ± 7.7	31.7 ± 7.7	K_{dPAR}
Kongsfjorden	0.93	41.5 ± 9.0	58.5 ± 9.0	PAR_{0-} (slightly)
Storfjorden	0.97	35.8 ± 8.2	64.2 ± 8.2	PAR_{0-}
Isfjorden	0.97	42.7 ± 7.7	57.3 ± 7.7	PAR_{0-} (slightly)
Porsangerfjorden	0.89	39.7 ± 8.7	60.3 ± 8.7	PAR_{0-}
Nuup Kangerlua	0.99	24.0 ± 7.1	76.0 ± 7.1	PAR_{0-}
Disko Bay	0.98	22.6 ± 6.4	77.4 ± 6.4	PAR_{0-}

Additionally, different dominant species, temperature-dependent growth rates (Smale et al. 2020), higher grazing pressure (Filbee-Dexter and Scheibling 2014), and the absence of ice-related disturbances in non-polar regions would also modify the irradiance-to-biomass relationship. Therefore, successfully transferring the model to non-Arctic regions would require adapting it to local underwater irradiance regimes and region-specific irradiance-to-biomass relationships.

Seafloor PAR as a predictor of kelp distribution

In the Arctic, the irradiance reaching the seafloor—or its indirect proxy, the number of open water days—has proven effective in mapping the kelp distribution (e.g., Krause-Jensen et al. 2020; Kvile et al. 2022; Castro de la Guardia et al. 2023). Our evaluation of the kelp distribution supports earlier studies by confirming $iPAR_b$ as a useful predictor of Arctic kelp presence (Lüning 1991; Gattuso et al. 2006; Attard et al. 2024). However, while $iPAR_b$ performed well in predicting kelp presence (e.g., high recall), relying on it alone can lead to overestimation, as reflected by the low specificity (Table 3). This limitation arises because our approach does not incorporate other key physical factors that constrain kelp distribution, such as hard substrata and temperature, with additional variables such as seawater salinity, nutrient availability and grazing playing secondary roles (Bluhm et al. 2022; Niedzwiedz and Bischof 2023). Incorporating these additional habitat layers, particularly substrata, which is not yet comprehensively mapped in the Arctic, could improve predictions of kelp distribution, and therefore warrants dedicated future research.

Seafloor PAR as a predictor of potential summer kelp biomass and standing stock in the lower depth range

Overall, the range in the predicted fjord-averaged summer biomass in the lower depth range across the seven Arctic fjords aligned closely with reported kelp summer biomass in the lower depth range in the Canadian Subarctic for the same assemblage of kelp species that we define as the kelp community (0.4 kg WW to 4.6 kg WW m^{-2}; Adey and Hayek 2011). In individual fjords, our predicted fjord-averaged biomass in the lower depth range was comparable in magnitude to full-depth averaged observations at Hansneset, Kongsfjorden (4.7 kg WW m^{-2}; Hop et al. 2016), but overestimated, by three times, the observed biomass in the lower depth range in Young Sound (0.02 kg WW m^{-2}; Borum et al. 2002). This overestimation may stem from our model predicting kelp community biomass (*A. esculenta*, *S. latissima*, and digitate kelps), while in Young Sound (or similar regions) there is only one common kelp species, *S. latissima* (Borum et al. 2002). Moreover, in Young Sound, the biomass, at any given depth, is more limited by hard substrata availability than by seafloor irradiance (Borum et al. 2002; Krause-Jensen et al. 2007).

The predicted potential spatial distribution of kelp biomass in the lower depth range within fjords followed the general observations of higher kelp biomass toward the middle and outer fjord in Kongsfjorden and Nuup Kangerlua, (Hop et al. 2016; Sejr et al. 2021). This spatial distribution is thought to reflect the decrease in irradiance due to increased turbidity near the terminus of tidewater glaciers with significant subglacial discharge, as the rising freshwater plume disturbs and disperses sediments. (e.g., Halbach et al. 2019; Meire et al. 2017; Inall et al. 2024). Prediction of potential kelp biomass in fjords with predominantly land runoff, Porsangerfjorden and Young Sound, was relatively low compared to fjords with marine terminating glaciers. These findings are consistent with observations by Gonzalez Triginer et al. (2024) of lower kelp cover associated with river surface outflows compared to subglacial outflows, because of less favorable light conditions due to the higher sedimentation rates near surface outflows. However, the amount of sediment in the fjords with subglacial discharge will also depend on glacier melt rates and bedrock characteristics (e.g., Meire et al. 2017; Halbach et al. 2019; Inall et al. 2024).

Our prediction of potential kelp standing stocks assumes 100% kelp cover on the seafloor within the lower depth range—an idealized upper limit used to define the maximum potential kelp standing stock. Such high kelp coverages are rare due to the patchy availability of hard substrata, the presence of grazers, and other limiting factors, all of which can significantly reduce kelp percentage cover even when irradiance conditions are optimal. In Young Sound, Kongsfjorden and Nuup Kangerlua, the observed averaged kelp cover from 0 to about 30 m is 36%, 45%, and 32%, respectively (Krause-Jensen et al. 2007; Hop et al. 2016; Kruss et al. 2017; Ager et al.

2023), demonstrating substantial and consistent deviation from our assumed 100% kelp cover across the studied fjords. Recent published data in eastern Greenland pooled observations from 64.5°N to 75.5°N, providing a large-scale average of kelp cover along a depth gradient (Wegeberg et al. 2025). If we assume the empirical kelp cover gradient reported by Wegeberg et al. (2025) applies to our fjords, then the predicted potential standing stock within the lower depth range shown in Fig. 4 would be reduced by approximately 40%.

Regular revisions of the empirical model as data become available may be required to adjust its parameters and the depth of maximum biomass. In the future and warmer Arctic, multiple biophysical interactions may change the shape of the relationship between $iPAR_b$ and summer biomass due to species-specific variability in irradiance levels required for survival in warmer and fresher coastal waters (Krause-Jensen et al. 2019; Niedzwiedz and Bischof 2023; Niedzwiedz et al. 2024; Diehl et al. 2024). Experimental evidence from Lebrun et al. (2024) indicates that *A. esculenta* is physiologically adapted to lower light and fresher conditions, enabling it to expand into deeper or more turbid habitats, whereas *S. latissima* and digitate kelps maintain more stable biomass across a broader range of light and salinity but may be outcompeted under very low irradiance. In the field, additional environmental drivers such as wave exposure, substrate type, and sedimentation rates interact with these physiological traits to alter competitive outcomes and modify the depth distribution of these kelps (Filbee-Dexter et al. 2022; Bluhm et al. 2022; Niedzwiedz and Bischof 2023; Düsedau et al. 2024a). This pattern is reflected in observations in Svalbard showing that as underwater light continues to decline, *A. esculenta* increasingly dominates darker habitats while *S. latissima* and digitate kelps persist until irradiance falls below their tolerance thresholds and remain at high biomass only in shallow (< 5 m) areas (Düsedau et al. 2024a; Miller et al. 2024; Filbee-Dexter pers. comm.). Consequently, as more adaptable species fill biomass gaps, the overall kelp community biomass may remain relatively stable. While changes in irradiance may not necessarily result in an increase in biomass or productivity, they can shift the depth distribution of biomass in the lower depth range (Düsedau et al. 2024a). Warming may also shift the depth distribution of biomass by stimulating colonization of kelp in shallower waters with less sea-ice scouring (Bartsch et al. 2016; Krause-Jensen et al. 2020; Düsedau et al. 2024a) and retreating glaciers (Ronowicz et al. 2020; Sejr et al. 2024).

Trends in turbidity and surface irradiance as drivers of seafloor PAR

As climate warming persists and intensifies, Arctic fjords may experience coastal darkening resulting in less optimal seafloor irradiance conditions due to increased turbidity associated with elevated runoff, the retreat of marine terminating glaciers, higher phytoplankton productivity, and coastal erosion, despite increases in incident irradiance due to loss of sea ice (e.g., Halbach et al. 2019; Maturilli et al. 2019; Singh et al. 2022). Our regionally averaged irradiance data in the lower depth range did not show evidence of increased turbidity between 2004 and 2022 (measured as remotely sensed K_{dPAR}) or surface irradiance (measured as remotely sensed PAR_{0-}). However, we found differences among the seven fjords in the relative contribution of K_{dPAR} and PAR_{0-} to the variance in seafloor irradiance, both annually integrated (e.g., $iPAR_b$) and annually averaged (e.g., PAR_b). These fjord-specific differences emphasize the complexity of seafloor irradiance conditions in the Arctic (Gattuso et al. 2006; Singh et al. 2022).

PAR_{0-} was the primary driver of the interannual variability in $iPAR_b$ in all fjords except Young Sound. This suggests a regionally dominant role of surface processes, sea ice and/or cloud cover, modulating PAR reaching the seafloor. This result does not exclude local processes, whereby increasing K_{PAR}, attributed to locally high runoff and glacier melt, has a dominant role driving the observed decline in seafloor irradiance (e.g., in Kongsfjorden, Düsedau et al. 2024a). Indeed, noting that in our GAM analysis for Kongsfjorden and Isfjorden the contribution of PAR_{0-} and K_{dPAR} was near equal (within 10%), which seems to capture a combination of increasing seafloor irradiance due to sea-ice loss and decreasing seafloor irradiance resulting from rising turbidity (Singh et al. 2022).

In Young Sound, a fjord without marine terminating glaciers, K_{dPAR} was the dominant driver of the interannual variability of $iPAR_b$. Land surface runoff in Young Sound is turbid, being strongly influenced by several main rivers fed by land terminating glaciers (Meire et al. 2017). Water turbidity explains over 80% of the variation of K_{dPAR} in Young Sound (Murray et al. 2015). The dominance of K_{dPAR} as a driver of $iPAR_b$ suggests that the future losses of sea ice cover due to warming and the associated potential increase of PAR_{0-} in this fjord may not bring much change to the underwater irradiance, which would parallel observations in Alaska (Bonsell and Dunton 2018). Consequently, we also do not expect much change in the extent of the kelp distribution or biomass as predicted in Young Sound. In contrast, variations in seafloor irradiance in Porsangerfjorden, a fjord without glaciers or sea ice and where freshwater discharged is heavily influenced by turbid runoff from land (Białogrodzka et al. 2018), were only secondarily dominated by K_{dPAR}. This could reflect the importance of cloud cover modulating surface ocean irradiance, and thus the variations in seafloor irradiance (Bélanger et al. 2012; Laliberté et al. 2021; Singh et al. 2022).

In general, the fjord waters had moderate turbidity within the area defined by the lower depth range of the potential kelp habitat. These estimates are similar to measured summer turbidity in near coastal waters of Storfjorden (mean 0.4 m^{-1}), Isfjorden (mean 0.3 m^{-1}) (Wiktor Jr et al. 2022), Young Sound (mean 0.4 m^{-1}) and Nuup Kangerlua (mean 0.4 m^{-1}) (Murray

et al. 2015). These K_{dPAR} values lie between the clear waters of non-fjord systems like in Northern Hudson Bay (mean K_{dPAR} 0.11 m^{-1}) where the kelp distribution aligned with the number of ice-free days with light (Castro de la Guardia et al. 2023), and the turbid waters of the Beaufort Sea Lagoons (mean $K_{dPAR} > 0.5\ m^{-1}$) where kelp distribution is already insensitive to the loss of sea ice (Bonsell and Dunton 2018). These results call for a continuum of careful assessment of the responses of K_{dPAR} to a warming climate in each fjord (Schlegel et al. 2024), as this may ultimately determine the fate of kelp distribution (Sejr et al. 2024) and greatly influence kelp primary productivity, even over short seasonal periods (Franke et al. 2023).

Comments and recommendations

Prediction of the potential Arctic kelp distribution, its summer biomass and standing stock can offer clearer insight into the role of kelp in the Arctic ecosystem and food webs. The novelty of our approach lies in providing temporally variable estimates of potential kelp distribution and biomass as a function of $iPAR_b$, a variable that responds to climate change. Although the empirical model developed here is specific to Arctic environments, the underlying framework is useful to non-Arctic regions. In temperate systems, where differences in temperature-dependent growth rates, higher grazing pressure, and the absence of ice-related disturbance would modify the irradiance-to–biomass relationship, the framework developed here can be adapted to local conditions. As research progresses in the domain of Arctic benthic ecology, our approach can be revised and refined, through updates of the irradiance-to-biomass empirical function and the incorporation and refinement of layers of growth-limiting factors to improve predictions of the kelp distribution. The development of autonomous underwater irradiance measurements in fjord systems, as well as the acquisition of detailed coastal substrata maps, will be key to improving mapping of macroalgal cover and potential biomass across the Arctic. Here we have shown that the combination of monitoring and modeling methods is a necessary step to gain a more complete understanding of the time frame for Arctic marine coastal ecosystems change.

Author Contributions

Laura Castro de la Guardia: Conceptualization (equal); formal analysis (lead); methodology (lead); visualization (lead); writing – original draft (lead); writing – review and editing (equal). **Inka Bartsch:** Conceptualization (equal); methodology (equal); writing – review and editing (equal). **Haakon Hop:** Methodology (equal); writing – review and editing (equal). **Sarina Niedzwiedz:** Visualization (equal); writing – review and editing (equal). **Luisa Düsedau:** Conceptualization (equal); writing – review and editing (equal). **Nora Diehl:** Writing – review and editing (equal). **Dorte Krause-Jensen:** Methodology (equal); writing – review and editing (equal). **Mikael Sejr:** Writing – review and editing (equal). **Thomas Gjerfluff Ager:** Writing – review and editing (equal). **Jean-Pierre Gattuso:** Conceptualization (equal); writing – review and editing (equal). **Robert W. Schlegel:** Methodology (equal); writing – review and editing (equal). **Cale A. Miller:** Writing – review and editing (equal). **Karen Filbee-Dexter:** Writing – review and editing (equal). **Pedro Duarte:** Conceptualization (equal); formal analysis (supporting); methodology (equal); funding acquisition; writing – original draft (supporting); writing – review and editing (equal); supervision.

Acknowledgments

We are thankful to Anaïs Lebrun for her contribution to earlier versions of this work, and the two expert reviewers for their detailed comments and constructive suggestions which helped improved the later version of this manuscript. This study was conducted in the scope of the European Union (EU) project FACE-IT (The Future of Arctic Coastal Environment—Identifying Transitions in Fjord Systems and Adjacent Coastal Areas). FACE-IT has received funding from the EU, managed by the European Comission, under its Horizon 2020 research and innovation program under the Grant Agreement No. 869154. It has also received funding from the *EU Horizon Europe Research and Innovation Programme,* managed by the European Comission under Grant Agreement No. 101136480 (SEA-Quester). Views and opinions expressed, however, are those of the author(s) and do not necessarily reflect those of the European Union, which implies that neither the European Union nor the grant authority can be held responsible for them. This research is supported by the Norwegian Research Council (NRC) project BlueARC (334760), and the NRC Centres of Excellence funding scheme to iC3: Centre for Ice, Cryosphere, Carbon and Climate (332635).

Conflicts of Interest

None declared.

Data Availability Statement

Data that support the analysis and findings in this study are openly available: (1) FjordLight dataset (K_{dPAR}, PAR_{0-}, PAR_b, and bathymetry) in Young Sound, Kongsfjorden, Storfjorden, Isfjorden, Porsangerfjorden, Nuup Kangerlua, Disko Bay (Gentili et al. 2023, 2024); (2) Kelp biomass of *Alaria esculenta*, *Saccharina latissima*, *Laminaria digitata* or digitate kelp along the depth gradient in Kongsfjorden in 1996/1998 (Hop et al. 2012b), 2012/2013 (cf. Tables S1 and S2 in Bartsch et al. 2016), and 2021 (Düsedau et al. 2024b); (3) GPS locations with the presence and absence of kelp in Young Sound, Kongsfjorden, Isfjorden, Porsangerfjorden and Nuup Kangerlua are submitted as TableS1.csv in this manuscript.

References

Adey, W. H., and L. A. C. Hayek. 2011. "Elucidating Marine Biogeography with Macrophytes: Quantitative Analysis of the North Atlantic Supports the Thermogeographic Model and Demonstrates a Distinct Subarctic Region in the Northwestern Atlantic." *Northeastern Naturalist* 18, no. MO8: 1–128. https://doi.org/10.1656/045.018.m801.

Ager, T. G., D. Krause-Jensen, B. Olesen, D. F. Carlson, M. H. S. Winding, and M. K. Sejr. 2023. "Macroalgal Habitats Support a Sustained Flux of Floating Biomass but Limited Carbon Export Beyond a Greenland Fjord." *Science of the Total Environment* 872: 162224. https://doi.org/10.1016/j.scitotenv.2023.162224.

Assis, J., E. A. Serrão, C. M. Duarte, E. Fragkopoulou, and D. Krause-Jensen. 2022. "Major Expansion of Marine Forests in a Warmer Arctic." *Frontiers in Marine Science* 9: 1–10. https://doi.org/10.3389/fmars.2022.850368.

Attard, K., R. K. Singh, J.-P. Gattuso, et al. 2024. "Seafloor Primary Production in a Changing Arctic Ocean." *Proceedings of the National Academy of Science* 121, no. 11: e2303366121. https://doi.org/10.1073/pnas.2303366121.

Bartsch, I., M. Paar, S. Fredriksen, et al. 2016. "Changes in Kelp Forest Biomass and Depth Distribution in Kongsfjorden, Svalbard, Between 1996–1998 and 2012–2014 Reflect Arctic Warming." *Polar Biology* 39: 2021–2036. https://doi.org/10.1007/s00300-015-1870-1.

Bélanger, S., M. Babin, and J.-É. Tremblay. 2012. "Increasing Cloudiness in Arctic Damps the Increase in Phytoplankton Primary Production Due to Sea Ice Receding." *Biogeosciences* 10: 4087–4101. https://doi.org/10.5194/bg-10-4087-2013.

Białogrodzka, J., M. Stramska, D. Ficek, and M. Wereszka. 2018. "Total Suspended Particulate Matter in the Porsanger Fjord (Norway) in the Summers of 2014 and 2015." *Oceanologia* 60, no. 1: 1–15. https://doi.org/10.1016/j.oceano.2017.06.002.

Bluhm, B. A., K. Brown, L. Rotermund, W. Williams, S. Danielsen, and E. C. Carmack. 2022. "New Distribution Records of Kelp in the Kitikmeot Region, Northwest Passage, Canada, Fill a Pan-Arctic Gap." *Polar Biology* 45: 719–736. https://doi.org/10.1007/s00300-022-03007-6.

Bonsell, C., and K. H. Dunton. 2018. "Long-Term Patterns of Benthic Irradiance and Kelp Production in the Central Beaufort Sea Reveal Implications of Warming for Arctic Inner Shelves." *Progress in Oceanography* 162: 160–170. https://doi.org/10.1016/j.pocean.2018.02.016.

Borum, J., M. Pedersen, D. Krause-Jensen, P. Christensen, and K. Nielsen. 2002. "Biomass, Photosynthesis and Growth of *Laminaria saccharina* in a High-Arctic Fjord, NE Greenland." *Marine Biology* 141: 11–19. https://doi.org/10.1007/s00227-002-0806-9.

Bringloe, T. T., D. P. Wilkinson, J. Goldsmit, et al. 2022. "Arctic Marine Forest Distribution Models Showcase Potentially Severe Habitat Losses for Cryophilic Species Under Climate Change." *Global Change Biology* 28: 3711–3727. https://doi.org/10.1111/gcb.16142.

Brown, M. B., M. S. Edwards, and K. Y. Kim. 2014. "Effects of Climate Change on the Physiology of Giant Kelp, *Macrocystis pyrifera*, and Grazing by Purple Urchin, *Strongylocentrotus purpuratus*." *Algae* 29: 203–215. https://doi.org/10.4490/algae.2014.29.3.203.

Castro de la Guardia, L., K. Filbee-Dexter, J. Reimer, et al. 2023. "Increasing Depth Distribution of Arctic Kelp With Increasing Number of Open Water Days with Light." *Elementa: Science of the Anthropocene* 11, no. 1: 00051. https://doi.org/10.1525/elementa.2022.00051.

Cesana, G. V., O. Pierpaoli, M. Ottaviani, L. Vu, Z. Jin, and I. Silber. 2024. "The Correlation Between Arctic Sea Ice, Cloud Phase and Radiation Using A-Train Satellites." *Atmospheric Chemistry and Physics* 24: 7899–7909. https://doi.org/10.5194/acp-24-7899-2024.

Chapman, A. R. O., and J. E. Lindley. 1980. "Seasonal Growth of *Laminaria solidungula* in the Canadian High Arctic in Relation to Irradiance and Dissolved Nutrient Concentrations." *Marine Biology* 57, no. 1: 1–5. https://doi.org/10.1007/BF00420961.

Christie, H., H. Gundersen, E. Rinde, et al. 2019. "Can Multitrophic Interactions and Ocean Warming Influence Large-Scale Kelp Recovery?" *Ecology and Evolution* 9: 2847–2862. https://doi.org/10.1002/ece3.4963.

Davies, T. W., and T. Smyth. 2025. "Darkening of the Global Ocean." *Global Change Biology* 31: e70227. https://doi.org/10.1111/gcb.70227.

Diehl, N., P. Laeseke, I. Bartsch, et al. 2024. "Photoperiod and Temperature Interactions Drive the Latitudinal Distribution of *Laminaria hyperborea* (Laminariales, Phaeophyceae) under Climate Change." *Journal of Phycology* 60: 1237–1255. https://doi.org/10.1111/jpy.13497.

Duarte, C. M. 1992. "Nutrient Concentration of Aquatic Plants: Patterns Across Species." *Limnology and Oceanography* 37: 882–889. https://doi.org/10.4319/lo.1992.37.4.0882.

Duarte, C. M., J. J. Middelburg, and N. Caraco. 2005. "Major Role of Marine Vegetation on the Oceanic Carbon Cycle." *Biogeosciences* 2: 1–8. https://doi.org/10.5194/bg-2-1-2005.

Dunton, K. H. 1990. "Growth and Production in *Laminaria solidungula*: Relation to Continuous Underwater Light Levels in the Alaskan High Arctic." *Marine Biology* 106, no. 2: 297–304. https://doi.org/10.1007/BF01314813.

Dunton, K. H., E. Reimnitz, and S. Schonberg. 1982. "An Arctic Kelp Community in the Alaskan Beaufort Sea." *Arctic* 35, no. 4: 457–571. https://doi.org/10.14430/arctic2355.

Düsedau, L., S. Fredriksen, M. Brand, et al. 2024a. "Kelp Forest Community Structure and Demography in Kongsfjorden (Svalbard) across 25 Years of Arctic Warming." *Ecology and Evolution* 14: e11606. https://doi.org/10.1002/ece3.11606.

Düsedau, L., S. Fredriksen, M. Brand, et al. 2024b. Mean Fresh Weight of Macroalgae Collected at Hansneset, Kongsfjorden, Spitsbergen in 2012, 2013 and 2021. PANGAEA. https://doi.org/10.1594/PANGAEA.964587.

Filbee-Dexter, K., K. A. MacGregor, C. Lavoie, et al. 2022. "Sea Ice and Substratum Shape Extensive Kelp Forests in the Canadian Arctic." *Frontiers in Marine Science* 9: 754074. https://doi.org/10.3389/fmars.2022.754074.

Filbee-Dexter, K., and R. E. Scheibling. 2014. "Sea Urchin Barrens as Alternative Stable States of Collapsed Kelp Ecosystems." *Marine Ecology Progress Series* 495: 1–25. https://doi.org/10.3354/meps10573.

Filbee-Dexter, K., T. Wernberg, S. Fredriksen, K. M. Norderhaug, and M. F. Pedersen. 2019. "Arctic Kelp Forests: Diversity, Resilience and Future." *Global and Planetary Change* 172: 1–14. https://doi.org/10.1016/j.gloplacha.2018.09.005.

Fossberg, J., S. Forbord, O. J. Broch, et al. 2018. "The Potential for Upscaling Kelp (*Saccharina latissima*) Cultivation in Salmon-Driven Integrated Multi-Trophic Aquaculture (IMTA)." *Frontiers in Marine Science* 5: 418. https://doi.org/10.3389/fmars.2018.00418.

Franke, K., L. C. Matthes, A. Graiff, U. Karsten, and I. Bartsch. 2023. "The Challenge of Estimating Kelp Production in a Turbid Marine Environment." *Journal of Phycology* 59: 518–537. https://doi.org/10.1111/jpy.13327.

Gattuso, J.-P., B. Gentili, C. M. Duarte, J. A. Kleypas, J. J. Middelburg, and D. Antoine. 2006. "Light Availability in the Coastal Ocean: Impact on the Distribution of Benthic Photosynthetic Organisms and their Contribution to Primary Production." *Biogeosciences* 3, no. 4: 489–513. https://doi.org/10.5194/bg-3-489-2006.

Gentili, B., R. K. Singh, S. Bélanger, R. Schlegel, and J.-P. Gattuso. 2023. FjordLight: PAR Data for Arctic Fjords. PANGAEA. https://doi.org/10.1594/PANGAEA.962895.

Gentili, B., R. K. Singh, S. Bélanger, R. Schlegel, and J.-P. Gattuso. 2024. FjordLight: Addendum to PAR Data for Arctic Fjords. PANGAEA. https://doi.org/10.1594/PANGAEA.965460.

Goldsmit, J., R. W. Schlegel, K. Filbee-Dexter, et al. 2021. "Kelp in the Eastern Canadian Arctic: Current and Future Predictions of Habitat Suitability and Cover." *Frontiers in Marine Science* 8: 1453. https://doi.org/10.3389/fmars.2021.742209.

Gonzalez Triginer, V., M. Beck, A. Sen, K. Bischof, and B. Damsgård. 2024. "Acoustic Mapping Reveals Macroalgal Settlement Following a Retreating Glacier Front in the High Arctic." *Frontiers in Marine Science* 11: 1438332. https://doi.org/10.3389/fmars.2024.1438332.

Graham, M. H., B. P. Kinlan, L. D. Druehl, L. E. Garske, and S. Banks. 2007. "Deep-Water Kelp Refugia as Potential Hotspots of Tropical Marine Diversity and Productivity." *Proceedings of the National Academy of Sciences* 104, no. 42: 16576–16580. https://doi.org/10.1073/pnas.0704778104.

Halbach, L., M. Vihtakari, P. Duarte, et al. 2019. "Tidewater Glaciers and Bedrock Characteristics Control the Phytoplankton Growth Environment in a Fjord in the Arctic." *Frontiers in Marine Science* 6: 254. https://doi.org/10.3389/fmars.2019.00254.

Hop, H., N. A. Kovaltchouk, and C. Wiencke. 2016. "Distribution of Macroalgae in Kongsfjorden, Svalbard." *Polar Biology* 39: 2037–2051. https://doi.org/10.1007/s00300-016-2048-1.

Hop, H., K. M. Norderhaug, T. Wernberg, et al. 2025. "Scientific Diving in Arctic Kelp Forest to Detect Climate-Related Changes." *Fram Forum* 14: 46–51. https://framforum.com.

Hop, H., C. Wiencke, B. Vögele, and N. A. Kovaltchouk. 2012a. "Species Composition, Zonation, and Biomass of Marine Benthic Macroalgae in Kongsfjorden, Svalbard." *Botanica Marina* 55, no. 4: 399–414. https://doi.org/10.1515/bot-2012-0097.

Hop, H., C. Wiencke, B. Vögele, and N. A. Kovaltchouk. 2012b. Fresh Biomass of Macroalgae Collected at Hansneset, Kongsfjorden, Spitsbergen in 1996/1998. PANGAEA. https://doi.org/10.1594/PANGAEA.864321.

Inall, M. E., A. Sundfjord, F. Cottier, et al. 2024. "Mixing, Water Transformation, and Melting Close to a Tidewater Glacier." *Geophysical Research Letters* 51: e2024GL108421. https://doi.org/10.1029/2024GL108421.

Jakobsson, M., L. A. Mayer, C. Bringensparr, et al. 2020. "The International Bathymetric Chart of the Arctic Ocean Version 4.0." *Scientific Data* 7: 176. https://doi.org/10.1038/s41597-020-0520-9.

Krause-Jensen, D., P. Archambault, J. Assis, et al. 2020. "Imprint of Climate Change on Pan-Arctic Marine Vegetation." *Frontiers in Marine Science* 7: 617324. https://doi.org/10.3389/fmars.2020.617324.

Krause-Jensen, D., and C. Duarte. 2016. "Substantial Role of Macroalgae in Marine Carbon Sequestration." *Nature Geoscience* 9: 737–774. https://doi.org/10.1038/ngeo2790.

Krause-Jensen, D., M. Kühl, P. B. Christensen, and J. Borum. 2007. "Benthic Primary Production in Young Sound, Northeast Greenland." In Carbon Cycling in Arctic Marine Ecosystems: Case Study Young Sound, edited by S. Rysgaard and R. N. Glud, vol. 58, 160–173. Meddelelser om Grønland-Bioscience.

Krause-Jensen, D., N. Marbà, B. Olesen, et al. 2012. "Seasonal Sea Ice Cover as Principal Driver of Spatial and Temporal Variation in Depth Extension and Annual Production of Kelp in Greenland." *Global Change Biology* 18: 2981–2994. https://doi.org/10.1111/j.1365-2486.2012.02765.x.

Krause-Jensen, D., M. K. Sejr, A. Bruhn, et al. 2019. "Deep Penetration of Kelps Offshore Along the West Coast of Greenland." *Frontiers in Marine Science* 6: 375. https://doi.org/10.3389/fmars.2019.00375.

Kruss, A., J. Tegowski, A. Tatarek, J. Wiktor, and P. Blondel. 2017. "Spatial Distribution of Macroalgae Along the Shores of Kongsfjorden (West Spitsbergen) Using Acoustic Imaging." *Polish Polar Research* 38, no. 2: 205–229. https://doi.org/10.1515/popore-2017-0009.

Kvile, K. Ø., G. S. Andersen, S. P. Baden, et al. 2022. "Kelp Forest Distribution in the Nordic Region." *Frontiers in Marine Science* 9: 850359. https://doi.org/10.3389/fmars.2022.850359.

Laliberté, J., S. Bélanger, and M. Babin. 2021. "Seasonal and Interannual Variations in the Propagation of Photosynthetically Available Radiation Through the Arctic Atmosphere." *Elementa: Science of the Anthropocene* 9, no. 1: 00083. https://doi.org/10.1525/elementa.2020.00083.

Lebrun, A., C. A. Miller, M. Meynadier, et al. 2024. "Multifactorial Effects of Warming, Low Irradiance, and Low Salinity on Arctic Kelps." *Biogeosciences* 21: 4605–4620. https://doi.org/10.5194/bg-21-4605-2024.

Lüning, K. 1991. "Seaweeds: Their Environment, Biogeography, and Ecophysiology." *Journal of the Marine Biological Association of the United Kingdom* 71, no. 1: 246. https://doi.org/10.1017/S0025315400037632.

Lüning, K., and M. J. Dring. 1979. "Continuous Underwater Light Measurement Near Helgoland (North Sea) and Its Significance for Characteristic Light Limits in the Sublittoral Region." *Helgoländer Wissenschaftliche Meeresuntersuchungen* 32: 403–424. https://doi.org/10.1007/BF02277985.

Makarov, V. N. 1998. "Raw Resources of Commercial Algae." In Commercial and Prospective Algae and Invertebrates of the Barents and White Seas (In Russian), edited by G. G. Mathishov, 257–277. Apatity.

Maturilli, M., I. Hanssen-Bauer, R. Neuber, M. Rex, and K. Edvardsen. 2019. "The Atmosphere Above Ny-Ålesund—Climate and Global Warming, Ozone and Surface UV Radiation." In The Ecosystem of Kongsfjorden, Svalbard, edited by H. Hop and C. Wiencke, 23–46. Cham: Springer International Publishing. https://doi.org/10.1007/978-3-319-46425-1_2.

Meire, L., J. Mortensen, P. Meire, et al. 2017. "Marine-Terminating Glaciers Sustain High Productivity in Greenland Fjords." *Global Change Biology* 23: 5344–5357. https://doi.org/10.1111/gcb.13801.

Miller, C. A., F. Gazeau, A. Lebrun, et al. 2024. "Productivity of Mixed Kelp Communities in an Arctic Fjord Exhibit Tolerance to a Future Climate." *Science of the Total Environment* 930: 172571. https://doi.org/10.1016/j.scitotenv.2024.172571.

Mohr, J. L., N. J. Wilimovsky, and E. Y. Dawson. 1957. "An Arctic Alaskan Kelp Bed." *Arctic* 10: 45–52. https://doi.org/10.14430/arctic3754.

Molis, M., F. Beuchel, J. Laudien, M. Włodarska-Kowalczuk, and C. Buschbaum. 2019. "Ecological Drivers of and Responses by Arctic Benthic Communities, With an Emphasis on Kongsfjorden, Svalbard." In The Ecosystem of Kongsfjorden, Svalbard. Advances in Polar Ecology, edited by H. Hop and C. Wiencke, 423–481. Cham: Springer International Publishing. https://doi.org/10.1007/978-3-319-46425-1_11.

Murray, C., S. Markager, C. A. Stedmon, T. Juul-Pedersen, M. K. Sejr, and A. Bruhn. 2015. "The Influence of Glacial Melt Water on Bio-Optical Properties in Two Contrasting Greenlandic Fjords." *Estuarine, Coastal and Shelf Science* 163: 72–83. https://doi.org/10.1016/j.ecss.2015.05.041.

Niedzwiedz, S., and K. Bischof. 2023. "Glacial Retreat and Rising Temperatures Are Limiting the Expansion of Temperate Kelp Species in the Future Arctic." *Limnology and Oceanography* 68: 816–830. https://doi.org/10.1002/lno.12312.

Niedzwiedz, S., T. Vonnahme, T. Juul-Pedersen, K. Bischof, and N. Diehl. 2024. "Light-Mediated Temperature Susceptibility of Kelp Species (*Agarum clathratum*, *Saccharina latissima*) in an Arctic Summer Heatwave Scenario." *Cambridge Prisms: Coastal Futures* 2: 1–40. https://doi.org/10.1017/cft.2024.5.

Plotkin, A. S., A. I. Railkin, E. I. Gerasimova, A. Y. Pimenov, and T. M. Sipenkova. 2005. "Subtidal Underwater Rock Communities of the White Sea: Structure and Interaction with Bottom Flow." *Russian Journal of Marine Biology* 31: 335–343. https://doi.org/10.1007/s11179-006-0001-9.

Ronowicz, M., M. Włodarska-Kowalczuk, and P. Kukliński. 2020. "Glacial and Depth Influence on Sublittoral Macroalgal Standing Stock in a High-Arctic Fjord." *Continental Shelf Research* 194: 104045. https://doi.org/10.1016/j.csr.2019.104045.

Schimani, K., K. Zacher, K. Jerosch, H. Pehlke, C. Wiencke, and I. Bartsch. 2022. "Video Survey of Deep Benthic Macroalgae and Macroalgal Detritus along a Glacial Arctic Fjord: Kongsfjorden (Spitsbergen)." *Polar Biology* 45: 1291–1305. https://doi.org/10.1007/s00300-022-03072-x.

Schlegel, R. W., R. K. Singh, B. Gentili, et al. 2024. "Underwater Light Environment in Arctic Fjords." *Earth System Science Data* 16: 2773–2788. https://doi.org/10.5194/essd-16-2773-2024.

Sejr, M. K., K. N. Mouritsen, D. Krause-Jensen, B. Olesen, M. E. Blicher, and J. Thyrring. 2021. "Small Scale Factors Modify Impacts of Temperature, Ice Scours and Waves and Drive Rocky Intertidal Community Structure in a Greenland Fjord." *Frontiers in Marine Science* 7: 607135. https://doi.org/10.3389/fmars.2020.607135.

Sejr, M. K., A. E. Poste, and P. E. Renaud. 2024. "Multiple Climatic Drivers Increase Pace and Consequences of Ecosystem Change in the Arctic Coastal Ocean." *Limnology and Oceanography Letters* 9: 683–695. https://doi.org/10.1002/lol2.10431.

Singh, R. K., A. Vader, C. J. Mundy, et al. 2022. "Satellite-Derived Photosynthetically Available Radiation at the Coastal Arctic Seafloor." *Remote Sensing* 14, no. 20: 5180. https://doi.org/10.3390/rs14205180.

Smale, D. A., A. Pessarrodona, N. King, et al. 2020. "Environmental Factors Influencing Primary Productivity of the Forest-Forming Kelp *Laminaria hyperborea* in the Northeast Atlantic." *Scientific Reports* 10, no. 1: 12161. https://doi.org/10.1038/s41598-020-69238-x.

Steneck, R. S., M. H. Graham, B. J. Bourque, et al. 2002. "Kelp Forest Ecosystems: Biodiversity, Stability, Resilience and Future." *Environmental Conservation* 29, no. 4: 436–459. https://doi.org/10.1017/S0376892902000322.

Tatarek, A., J. Wiktor, and M. A. Kendall. 2012. "The Sublittoral Macroflora of Hornsund." *Polar Research* 31: 18900. https://doi.org/10.3402/polar.v31i0.18900.

Teagle, H., S. J. Hawkins, P. J. Moore, and D. A. Smale. 2017. "The Role of Kelp Species as Biogenic Habitat Formers in Coastal Marine Ecosystems." *Journal of Experimental Marine Biology and Ecology* 492: 81–98. https://doi.org/10.1016/j.jembe.2017.01.017.

Traiger, S. A., S. T. McKinney, and P. Gibbons. 2019. "Effects of Elevated Temperature and Sedimentation on Grazing Rates of the Green Sea Urchin: Implications for Kelp Forests Exposed to Increased Sedimentation with Climate Change." *Helgoland Marine Research* 73, no. 5: 1–7. https://doi.org/10.1186/s10152-019-0526-x.

Wang, X., J. Liu, B. Yang, et al. 2021. "Seasonal Trends in Clouds and Radiation Over the Arctic Seas From Satellite Observations during 1982 to 2019." *Remote Sensing* 13, no. 6: 3201. https://doi.org/10.3390/rs13163201.

Wegeberg, S., J. Wiktor Jr., J. F. Linnebjerg, and O. Geertz-Hansen. 2025. "Latitude, Sea Ice, and Glaciers Are Important Drivers of Submerged Vegetation Distributions in the Arctic Coastal Waters Along East Greenland." *Limnology and Oceanography* 70, no. 6: 1575–1590. https://doi.org/10.1002/lno.70056.

Wernberg, T., K. Krumhansl, K. Filbee-Dexter, and M. F. Pedersen. 2019. "Status and Trends for the World's Kelp Forests." In World Seas: An Environmental Evaluation, edited by C. Sheppard, 57–78. Academic Press. https://doi.org/10.1016/B978-0-12-805052-1.00003-6.

Wiencke, C., and C. D. Amsler. 2012. "Seaweeds and Their Communities in Polar Regions." In Seaweed Biology, Ecological Studies 219, edited by C. Wiencke and K. Bischof. Berlin Heidelberg: Springer-Verlag. https://doi.org/10.1007/978-3-642-28451-9_13.

Wiktor, J. M., Jr., A. Tatarek, A. Kruss, R. K. Singh, J. M. Wiktor, and J. E. Søreide. 2022. "Comparison of Macroalgae Meadows in Warm Atlantic Versus Cold Arctic Regimes in the High-Arctic Svalbard." *Frontiers in Marine Science* 9: 1021675. https://doi.org/10.3389/fmars.2022.1021675.

Wright, L. S., A. Pessarrodona, and A. Foggo. 2022. "Climate-Driven Shifts in Kelp Forest Composition Reduce Carbon Sequestration Potential." *Global Change Biology* 28: 5514–5531. https://doi.org/10.1111/gcb.16299.

Zacher, K., M. Bernard, I. Bartsch, and C. Wiencke. 2016. "Survival of Early Life History Stages of Arctic Kelps (Kongsfjorden, Svalbard) Under Multifactorial Global Change Scenarios." *Polar Biology* 39: 2009–2020. https://doi.org/10.1007/s00300-016-1906-1.

Supporting Information

Additional Supporting Information may be found in the online version of this article.

Submitted 12 May 2025
Revised 10 November 2025
Accepted 17 November 2025